(12) UK Patent Application (19) GB (11) 2 398 920 (13) A

(43) Date of A Publication 01.09.2004

(21) Application No: 0401758.8

(22) Date of Filing: 28.01.2004

(30) Priority Data:
(31) 2003048688 (32) 26.02.2003 (33) JP

(71) Applicant(s):
Alps Electric Co., Ltd.
(Incorporated in Japan)
1-7 Yukigaya, Otsuka-cho, Ota-ku,
Tokyo 145, Japan

(72) Inventor(s):
Naoya Hasegawa
Eiji Umetsu
Masamichi Saito
Yokuki Ide

(74) Agent and/or Address for Service:
Saunders & Dolleymore
9 Rickmansworth Road, WATFORD, Herts,
WD18 0JU, United Kingdom

(51) INT CL[7]:
G11B 5/39

(52) UK CL (Edition W):
G5R RMMT

(56) Documents Cited:
US 5920446 A US 5648885 A
US 20020044398 A1

(58) Field of Search:
UK CL (Edition W) G5R
INT CL[7] G01R, G11B
Other: Online: EPODOC, WPI, PAJ

(54) Abstract Title: **Spin valve magnetoresistive element**

(57) A first magnetic sublayer 23a of a pinned magnetic layer 23 is formed on a nonmagnetic metal layer 22. The nonmagnetic metal layer is composed of at least one element selected from the group consisting of Ru, Re, Os, Ti, Rh, Ir, Pd, Pt, and Al. The atoms in the first magnetic sublayer and the atoms in the nonmagnetic metal layer are epitaxial and overlapped with each other, while each of the crystal structures is deformed. The deformations in the crystal structure of the first magnetic sublayer increase the magnetostriction constant, thereby providing a magnetic sensor having a large magnetoelastic effect.

FIG. 1

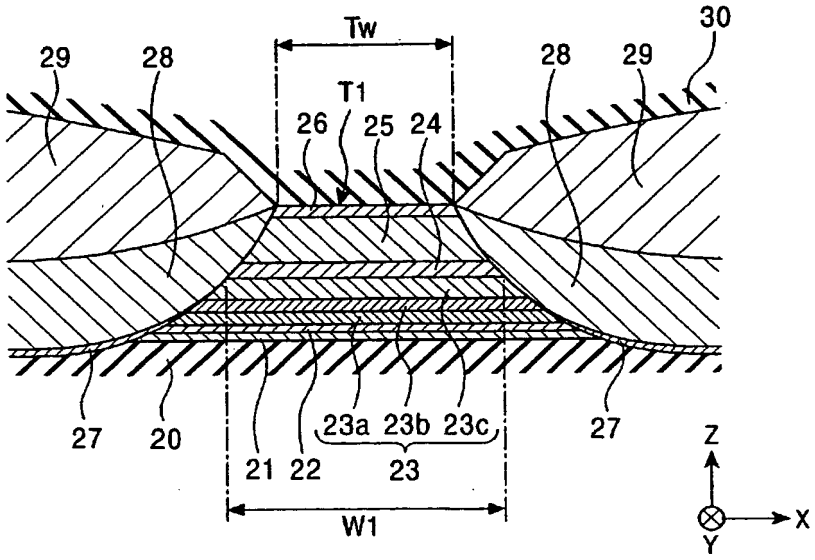

GB 2 398 920 A

FIG. 1

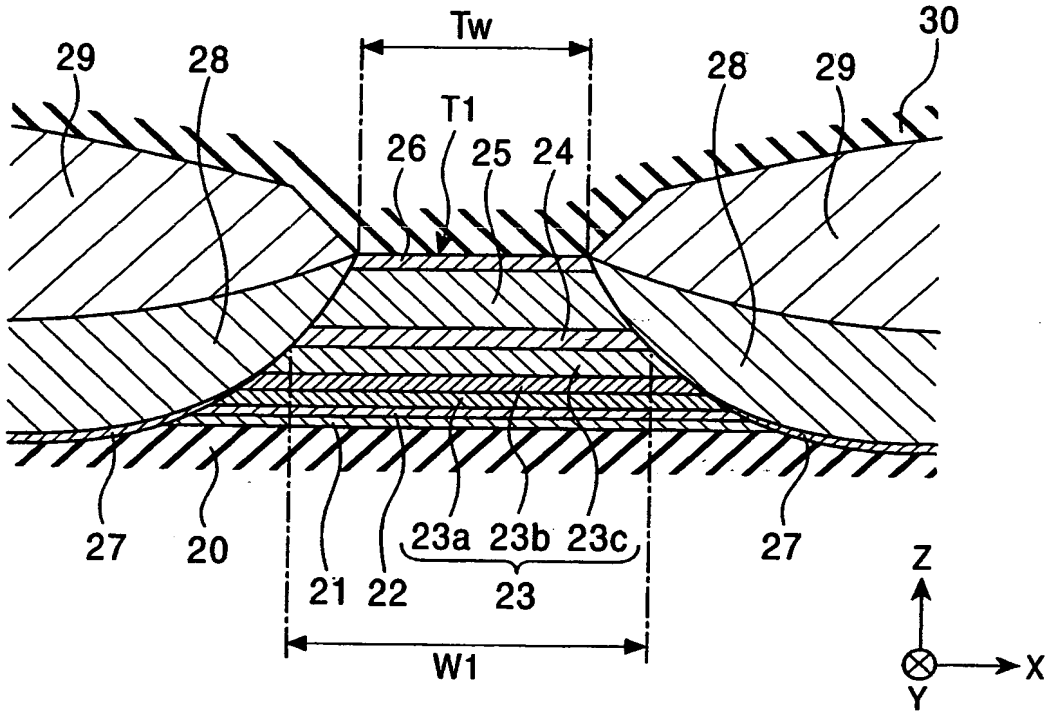

FIG. 2

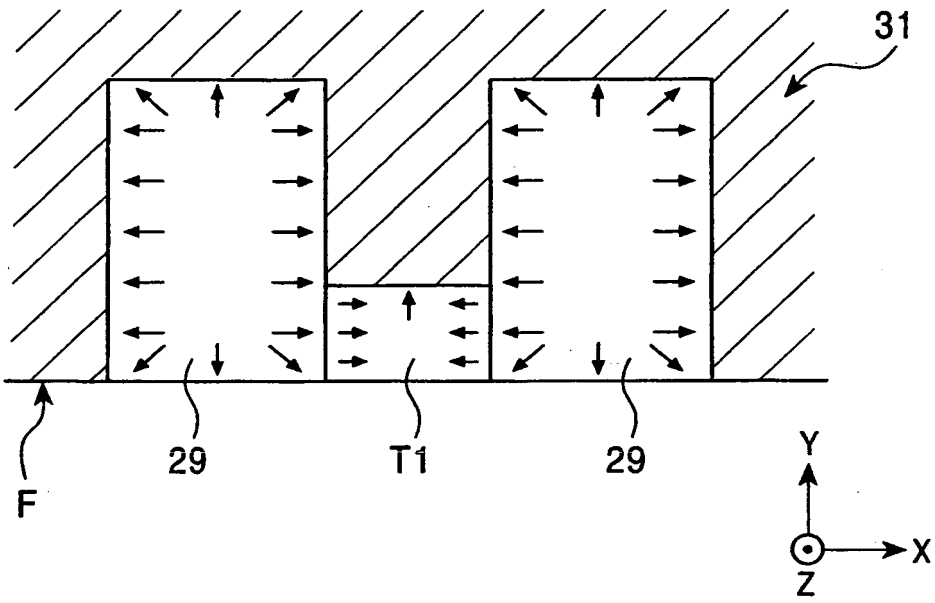

FIG. 3

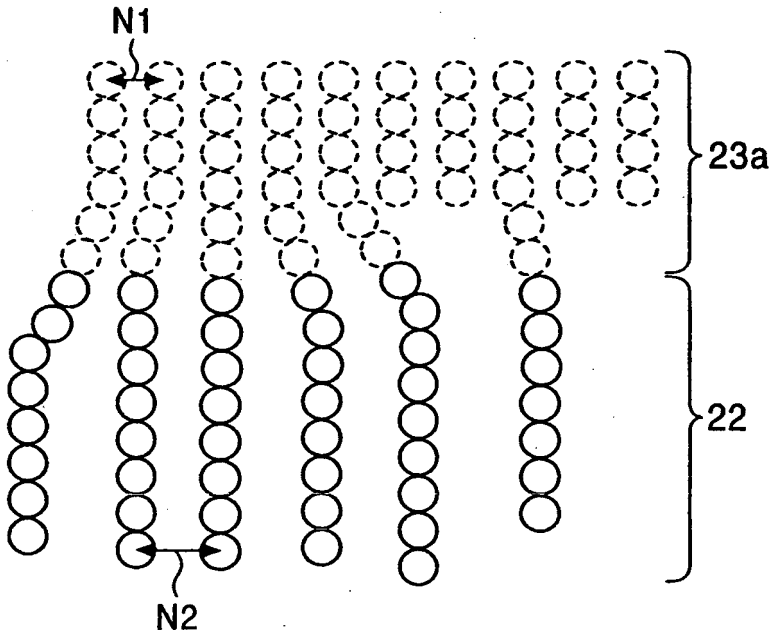

FIG. 4

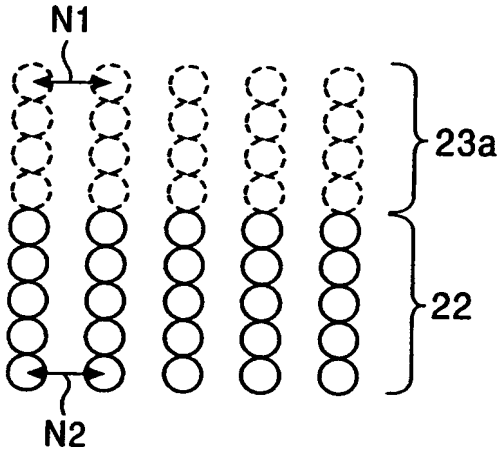

FIG. 5

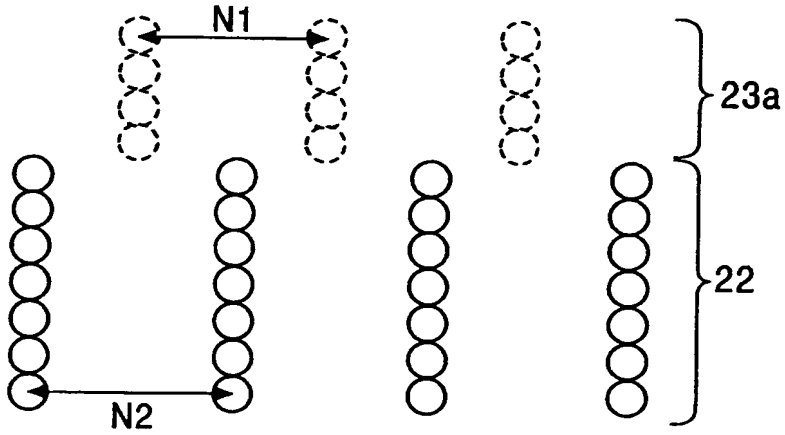

FIG. 6

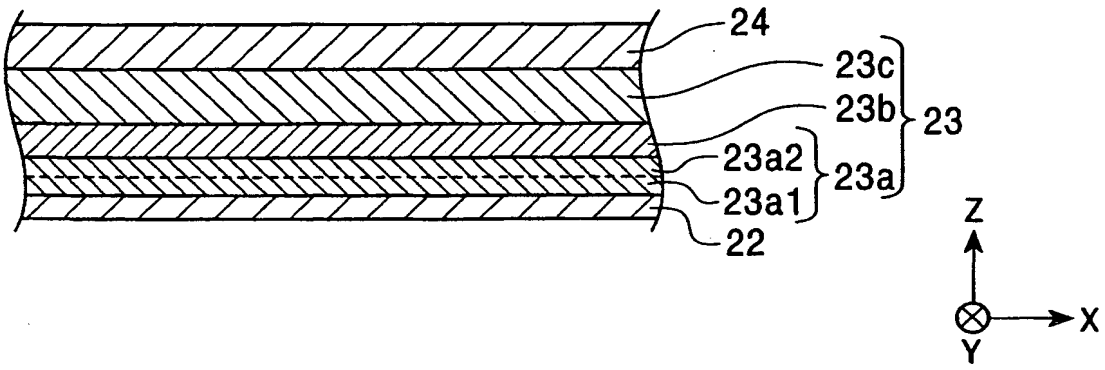

FIG. 7

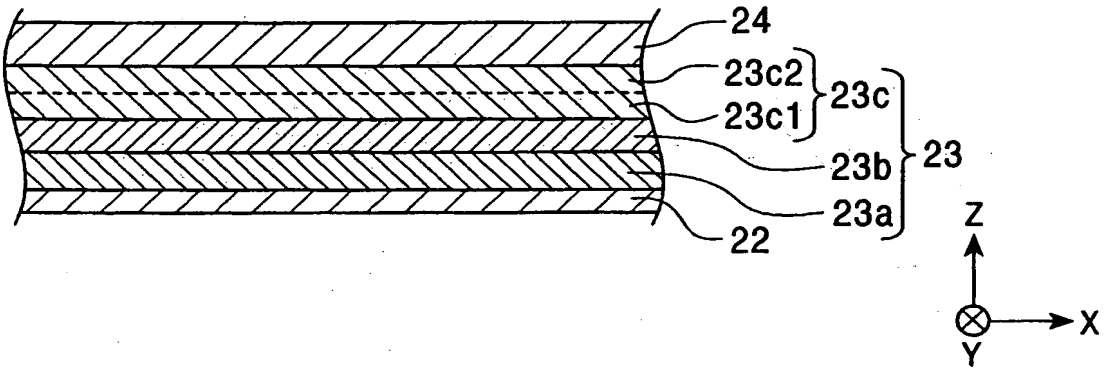

FIG. 8

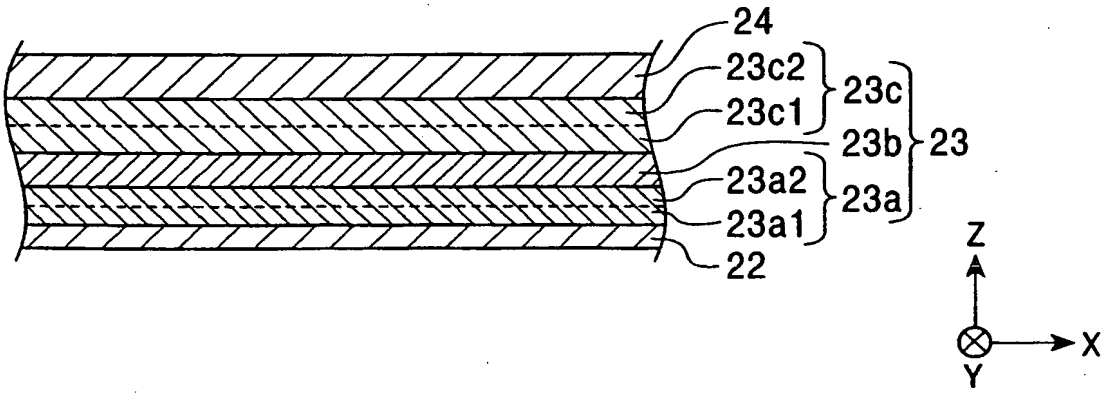

FIG. 9

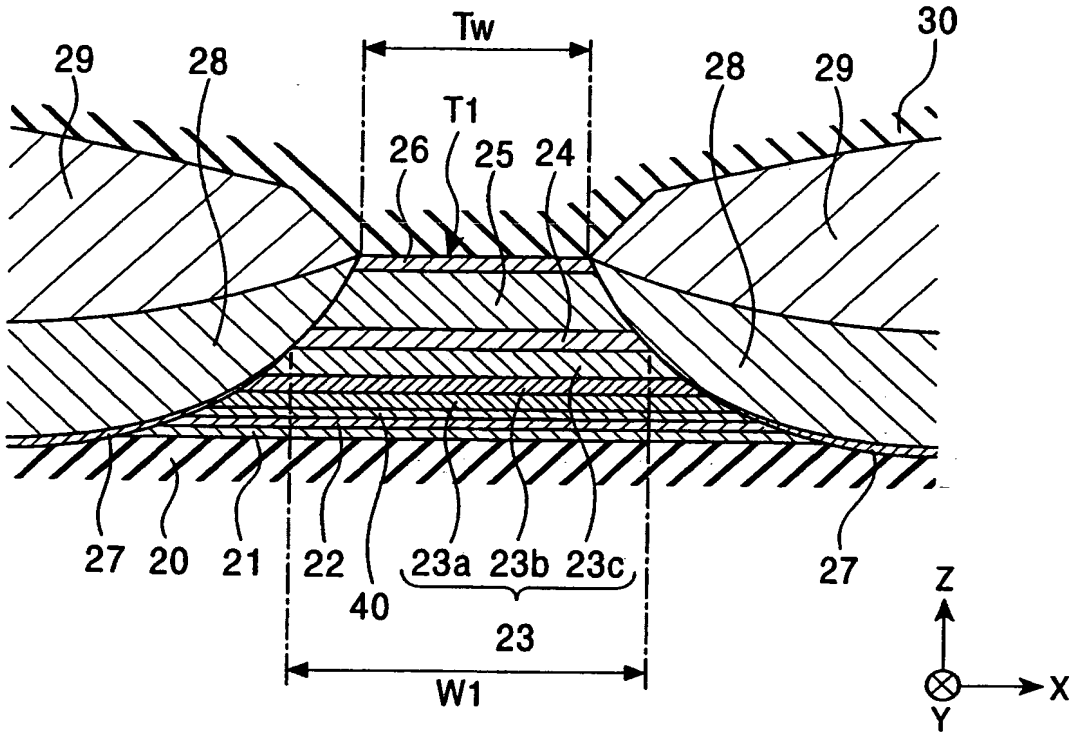

FIG. 10

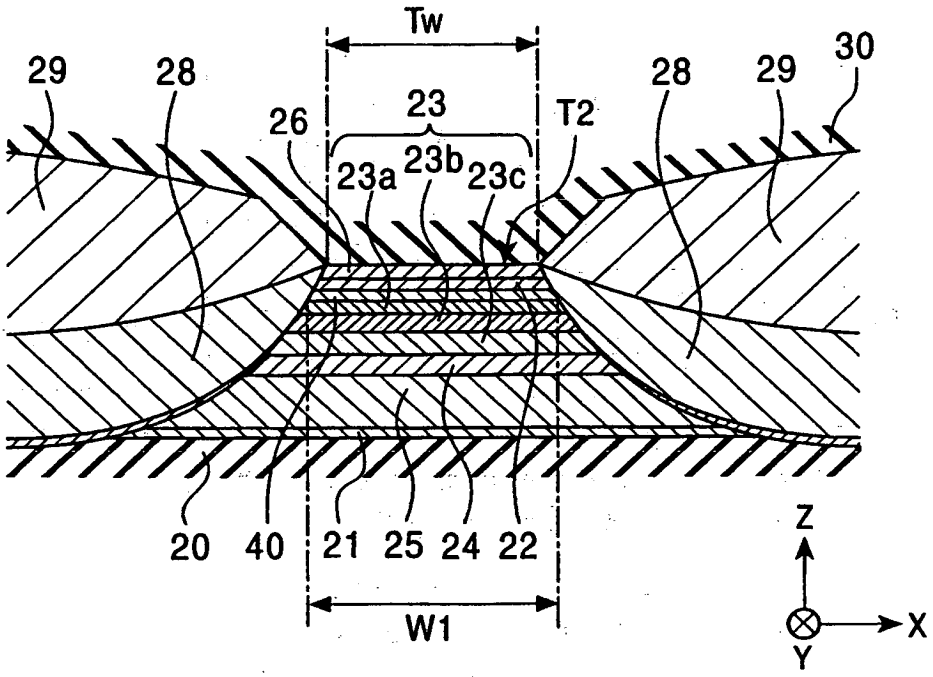

FIG. 11

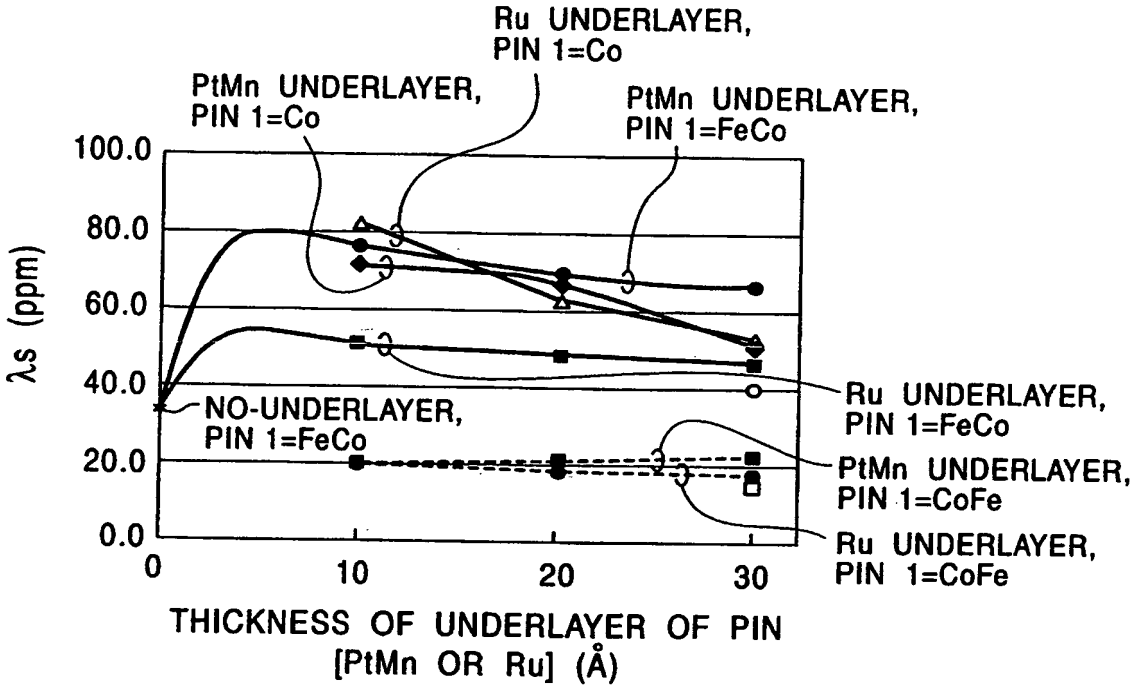

- PtMn UNDERLAYER, PIN 1=Co (22), PIN 2=Co (40)
- Ru UNDERLAYER, PIN 1=Co (22), PIN 2=Co (40)
- PtMn UNDERLAYER, PIN 1= CoFe (24), PIN 2= CoFe (40)
- PtMn UNDERLAYER, PIN 1= CoFe (18), PIN 2= CoFe (40)
- Ru UNDERLAYER, PIN 1= CoFe (24), PIN 2= CoFe (40)
- NO-UNDERLAYER PIN 1=FeCo(16), PIN 2=Co(40)
- PtMn UNDERLAYER, PIN 1= FeCo (16), PIN 2=Co (40)
- Ru UNDERLAYER, PIN 1= FeCo (16), PIN 2=Co (40)
- Ru UNDERLAYER, PIN 1= FeCo (12), PIN 2=Co (40)

(NUMERALS IN PARENTHESES REPRESENT FILM THICKNESS Å)

FIG. 12
PRIOR ART

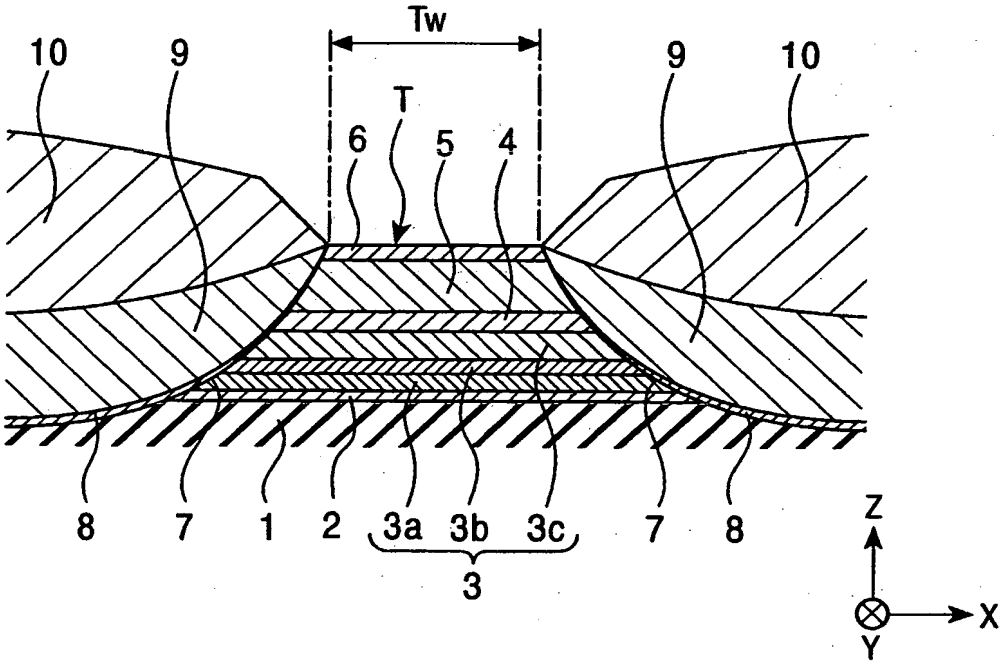

SPIN VALVE MAGNETORESISTIVE ELEMENT

BACKGROUND OF THE INVENTION

1. Field of the Invention

The present invention relates to a magnetic sensor having a free magnetic layer, a nonmagnetic conductive layer, and a pinned magnetic layer, and in particular, to a magnetic sensor that pins the magnetization of the pinned magnetic layer by means of a uniaxial anisotropy of the pinned magnetic layer itself.

2. Description of the Related Art

Recently, most magnetic heads mounted in magnetic recording and playback devices include a spin valve magnetic sensor that uses the giant magnetoresistive (GMR) effect.

The spin valve magnetic sensor includes a ferromagnetic film called a pinned magnetic layer, a ferromagnetic soft magnetic film called a free magnetic layer, and a nonmagnetic film called a nonmagnetic conductive layer. The nonmagnetic conductive layer is disposed between the pinned magnetic layer and the free magnetic layer.

The magnetization of the free magnetic layer is aligned in one direction by a longitudinal bias magnetic field from, for example, a hard bias layer composed of a hard magnetic material. The magnetization of the free magnetic layer is sensitively changed in response to an external magnetic field generated from a recording medium. On the other hand, the

magnetization of the pinned magnetic layer is pinned in a direction that crosses with the magnetization direction of the free magnetic layer.

The relationship between the changes of magnetization direction of the free magnetic layer and the pinned magnetization direction of the pinned magnetic layer changes the electrical resistance. A leakage field from the recording medium is detected by changes of voltage or current based on the change of the electrical resistance.

In the known art, the pinned magnetic layer is formed on an antiferromagnetic layer composed of an antiferromagnetic material such as PtMn. An exchange coupling magnetic field is created between the pinned magnetic layer and the antiferromagnetic layer, thereby pinning the magnetization of the pinned magnetic layer.

The exchange coupling magnetic field generated at the boundary face between the antiferromagnetic layer and the pinned magnetic layer can be large enough to prevent the change of the magnetization direction of the pinned magnetic layer, due to the application of a magnetic field during the manufacturing process or a leakage field from the recording medium. Furthermore, the antiferromagnetic layer itself does not generate an external magnetic field; therefore, this structure simplifies the design of the magnetic sensor.

However, the antiferromagnetic layer must have a thickness of about 200 Å so that the exchange coupling magnetic field generated at the boundary face between the antiferromagnetic layer and the pinned magnetic layer has a

sufficient intensity.

An antiferromagnetic layer having a large thickness disposed in the laminated component of a magnetic sensor mainly causes a shunt loss of a sense current. In order to achieve a high recording density on the recording medium, the output of the magnetic sensor must be improved. However, the shunt loss of the sense current prevents improvement of the output of the magnetic sensor.

Furthermore, shield layers composed of a soft magnetic material are disposed on the magnetic sensor and under the magnetic sensor in order to effectively read recording signals to be detected. In order to achieve a high linear recording density on the recording medium, the distance between the top shield layer and the bottom shield layer must be small. An antiferromagnetic layer having a large thickness prevents the distance between the top shield layer and the bottom shield layer being small.

Referring to Fig. 12, a magnetic sensor that does not have the antiferromagnetic layer has been proposed. The magnetic sensor pins the magnetization of the pinned magnetic layer by means of a uniaxial anisotropy of the pinned magnetic layer itself.

The magnetic sensor shown in Fig. 12 include a multilayer film T having, from the bottom, a bottom gap layer 1, an underlayer 2, a pinned magnetic layer 3 having a synthetic ferrimagnetic structure, a nonmagnetic conductive layer 4, a free magnetic layer 5, and a protective layer 6 in that order. The pinned magnetic layer 3 includes a first

magnetic sublayer 3a, a second magnetic sublayer 3c, and a nonmagnetic interlayer 3b disposed therebetween. Furthermore, at both sides 7 of the multilayer film T, bias base layers 8, hard bias layers 9, and electrode layers 10 are formed.

The magnetic sensor shown in Fig. 12 does not have the antiferromagnetic layer that is overlapped with the pinned magnetic layer 3. According to this magnetic sensor, the magnetization of the pinned magnetic layer 3 is pinned in the Y direction shown in the figure by means of the uniaxial anisotropy of the pinned magnetic layer 3 itself. Accordingly, the shunt loss can be small compared with a known magnetic sensor having the antiferromagnetic layer. Thus, the output in detecting the magnetic field of the magnetic sensor can be improved by 20% to 30%. Furthermore, the distance between the top shield layer and the bottom shield layer, which are disposed on and under the magnetic sensor, respectively, can be small, thereby achieving a higher linear recording density on the recording medium.

Japanese Unexamined Patent Application Publication Nos. 8-7235 (pp. 8 and 9, Fig. 5) and 2000-113418 (pp. 7 and 8, Figs. 4, 5, 6, and 7) disclose the magnetic sensor shown in Fig. 12.

The magnetic sensor described in Japanese Unexamined Patent Application Publication No. 8-7235 includes a buffer layer 62, i.e., an underlayer, composed of tantalum (Ta), and a pinned ferromagnetic layer 70 disposed thereon. The pinned ferromagnetic layer 70 includes a first cobalt (Co) film 72, a second cobalt (Co) film 74, and a ruthenium (Ru) film 73

disposed therebetween. The magnetization of the first cobalt (Co) film 72 and the second cobalt (Co) film 74 is pinned by each of the anisotropy fields. The first cobalt (Co) film 72 and the second cobalt (Co) film 74 are antiferromagnetically bonded to each other. The first cobalt (Co) film 72 and the second cobalt (Co) film 74 are magnetized in antiparallel directions.

As described above, the magnetic sensor described in Japanese Unexamined Patent Application Publication No. 8-7235 includes the buffer layer composed of tantalum having cobalt (Co) films thereon. Unfortunately, this structure cannot appropriately pin the magnetization direction of the pinned ferromagnetic layer 70. Japanese Unexamined Patent Application Publication No. 2000-113418 also points out this problem.

The magnetic sensor described in Japanese Unexamined Patent Application Publication No. 2000-113418 was invented in order to solve the problem in Japanese Unexamined Patent Application Publication No. 8-7235. According to this magnetic sensor, ferromagnetic layers in a laminated ferrimagnetic pinned layer are composed of CoFe or CoFeNi, thereby improving the induced anisotropy.

Furthermore, Japanese Unexamined Patent Application Publication No. 2000-113418 discloses an underlayer composed of Ta, the underlayer being disposed under the laminated ferrimagnetic pinned layer. Referring to experimental results in which the presence of the Ta underlayer is compared (see Figs. 4, 5, 6, and 7 in Japanese Unexamined

Patent Application Publication No. 2000-113418), when using CoFe alloy as the ferromagnetic layers, a magnetic sensor that does not have the Ta underlayer has a larger magnetoresistance change and a larger coercive force than those of the magnetic sensor that has the Ta underlayer.

In Japanese Unexamined Patent Application Publication No. 2000-113418, CoFe alloy is used as the ferromagnetic layers, and the ferromagnetic layers have a positive magnetostriction in order to increase the induced anisotropy of the laminated ferrimagnetic pinned layer.

The most important factor to pin the magnetization of the self-pinning type pinned magnetic layer is the uniaxial anisotropy due to magnetoelastic energy of the pinned magnetic layer. In particular, it is important to optimize the magnetostriction of the pinned magnetic layer. However, Japanese Unexamined Patent Application Publication No. 2000-113418 does not disclose a consideration relating to the mechanism to optimize the magnetostriction of the pinned magnetic layer. Also, the patent document does not disclose a specific construction to optimize the magnetostriction of the pinned magnetic layer.

SUMMARY OF THE INVENTION

In order to solve the above problems, it is an object of the present invention to provide a magnetic sensor having a self-pinning type pinned magnetic layer, the magnetic sensor strongly pinning the magnetization of the pinned magnetic layer. In the present invention, the mechanism to control

the magnetostriction of the pinned magnetic layer is made clear, and the material of a nonmagnetic metal layer that is in contact with the pinned magnetic layer is appropriately selected in order to appropriately regulate the magnetostriction.

The present invention provides a magnetic sensor including a pinned magnetic layer, a free magnetic layer, and a nonmagnetic conductive layer disposed therebetween, wherein the pinned magnetic layer includes a plurality of laminated magnetic sublayers having a nonmagnetic interlayer therebetween; a first magnetic sublayer of the plurality of the magnetic sublayers is disposed farthest from the nonmagnetic conductive layer, and is in contact with a nonmagnetic metal layer composed of at least one element selected from the group consisting of Ru, Re, Os, Ti, Rh, Ir, Pd, Pt, and Al; the crystals in the nonmagnetic metal layer and the crystals in the first magnetic sublayer are oriented in an epitaxial or a heteroepitaxial state; and an end face of the pinned magnetic layer is opened, the end face opposing a face of a recording medium.

The magnetic sensor of the present invention does not have an antiferromagnetic layer that is overlapped with the pinned magnetic layer, and the magnetization of the pinned magnetic layer is pinned by means of the uniaxial anisotropy of the pinned magnetic layer itself. That is, the magnetic sensor of the present invention is a self-pinning type magnetic sensor.

Accordingly, the shunt loss can be small compared with a

known magnetic sensor having the antiferromagnetic layer. Thus, the output in detecting the magnetic field of the magnetic sensor can be improved by 20% to 30%. Furthermore, the distance between a top shield layer and a bottom shield layer, which are disposed on and under the magnetic sensor, respectively, can be small, thereby achieving a higher linear recording density on the recording medium.

The factors that determine a magnetic anisotropy-magnetic field of a ferromagnetic layer include a crystal magnetic anisotropy, an induced magnetic anisotropy and a magnetoelastic effect. With regard to the crystal magnetic anisotropy, it is difficult to arrange the anisotropy uniaxially in a layer having crystals in which polycrystals orient at random. On the other hand, with regard to the induced magnetic anisotropy, the uniaxis is obtained by applying a magnetic field in one direction during deposition or heat treatment, and with regard to the magnetoelastic effect, the uniaxis is obtained by applying a uniaxial stress.

The uniaxial anisotropy to pin the magnetization of the pinned magnetic layer is determined by the induced magnetic anisotropy and the magnetoelastic effect. The present invention has achieved by paying attention to the magnetoelastic effect.

The magnetoelastic effect is controlled by magnetoelastic energy. The magnetoelastic energy is defined by the stress on the pinned magnetic layer and the magnetostriction constant of the pinned magnetic layer.

According to the present invention, an end face of the

pinned magnetic layer is opened, the end face opposing a face of a recording medium. Accordingly, the symmetry of the stress is lost, and a tensile strength is applied to the pinned magnetic layer in the height direction of the sensor (the height direction, or the direction of the normal line to the opposing face).

According to the present invention, the increase of the magnetostriction constant of the pinned magnetic layer increases the magnetoelastic energy, thereby increasing the uniaxial anisotropy of the pinned magnetic layer. The increase of uniaxial anisotropy of the pinned magnetic layer allows the magnetization of the pinned magnetic layer to be strongly pinned in one direction. Furthermore, the increase of uniaxial anisotropy of the pinned magnetic layer increases the output of the magnetic sensor and improves the output stability and the symmetry.

Specifically, the first magnetic sublayer, which is one of the plurality of magnetic layers of the pinned magnetic layer, is bonded with the nonmagnetic metal layer composed of at least one element selected from the group consisting of Ru, Re, Os, Ti, Rh, Ir, Pd, Pt, and Al such that the first magnetic sublayer and the nonmagnetic metal layer are oriented in an epitaxial or a heteroepitaxial state. Thus, deformation occurs in the crystal structure of the first magnetic sublayer, thereby increasing the magnetostriction constant λ of the first magnetic sublayer.

When the nonmagnetic metal layer is composed of at least one element selected from the group consisting of Rh, Ir, Pd,

Pt, and Al, the nonmagnetic metal layer preferably has a face-centered cubic (fcc) lattice structure in the vicinity of a boundary face adjacent to the first magnetic sublayer of the pinned magnetic layer or in the entire areas of the nonmagnetic metal layer, an equivalent crystal plane represented by a {111} plane being preferentially oriented in the direction parallel to the boundary face.

When the nonmagnetic metal layer is composed of at least one element selected from the group consisting of Ru, Re, Os, and Ti, the nonmagnetic metal layer preferably has a hexagonal close-packed (hcp) structure in the vicinity of a boundary face adjacent to the first magnetic sublayer of the pinned magnetic layer or in the entire areas of the nonmagnetic metal layer, a C-plane ({0001} plane) being preferentially oriented in the direction parallel to the boundary face.

Bias layers to supply the free magnetic layer with a longitudinal bias magnetic field are preferably formed at both side ends of the free magnetic layer and the pinned magnetic layer.

According to the present invention, the first magnetic sublayer of the pinned magnetic layer preferably has a face-centered cubic (fcc) lattice structure in the vicinity of a boundary face adjacent to the nonmagnetic metal layer or in the entire areas of the first magnetic sublayer, an equivalent crystal plane represented by a {111} plane being preferentially oriented in the direction parallel to the boundary face.

As described above, the nonmagnetic metal layer of the present invention has the fcc structure, and an equivalent crystal plane represented by the {111} plane being preferentially oriented in the direction parallel to the boundary face. Alternatively, the nonmagnetic metal layer has the hcp structure, and the C-plane being preferentially oriented in the direction parallel to the boundary face.

Accordingly, when the first magnetic sublayer has the fcc structure, and an equivalent crystal plane represented by the {111} plane being preferentially oriented in the direction parallel to the boundary face, the atoms in the first magnetic sublayer and the atoms in the nonmagnetic metal layer are readily overlapped with each other.

However, there is a certain amount of difference between the nearest interatomic distance in the {111} plane of the first magnetic sublayer and the nearest interatomic distance in the {111} plane or in the C-plane of the nonmagnetic metal layer. Accordingly, in the vicinity of the boundary face between the first magnetic sublayer and the nonmagnetic metal layer, the atoms in the first magnetic sublayer and the atoms in the nonmagnetic metal layer are overlapped with each other, while each of the crystal structures is deformed. Thus, the generation of the deformations in the crystal structure of the first magnetic sublayer can increase the magnetostriction constant λ.

For example, when the first magnetic sublayer of the pinned magnetic layer is composed of Co or Co_xFe_y ($20 \geq y$, $x+y=100$, and wherein each of x and y is represented as an

atomic percent), the first magnetic sublayer preferably has an fcc structure, an equivalent crystal plane represented by a {111} plane being preferentially oriented in the direction parallel to the boundary face.

Alternatively, the first magnetic sublayer of the pinned magnetic layer preferably has a body-centered cubic (bcc) lattice structure in the vicinity of a boundary face adjacent to the nonmagnetic metal layer or in the entire areas of the first magnetic sublayer, an equivalent crystal plane represented by a {110} plane being preferentially oriented in the direction parallel to the boundary face.

Even when the first magnetic sublayer has the bcc structure, an equivalent crystal plane represented by the {110} plane being preferentially oriented in the direction parallel to the boundary face, the atoms in the first magnetic sublayer and the atoms in the nonmagnetic metal layer are readily overlapped with each other.

In this case, there is also a certain amount of difference between the nearest interatomic distance in the {110} plane of the first magnetic sublayer and the nearest interatomic distance in the {111} plane or in the C-plane of the nonmagnetic metal layer. Accordingly, in the vicinity of the boundary face between the first magnetic sublayer and the nonmagnetic metal layer, the atoms in the first magnetic sublayer and the atoms in the nonmagnetic metal layer are overlapped with each other, while each of the crystal structures is deformed. Thus, the generation of the deformations in the crystal structure of the first magnetic

sublayer can increase the magnetostriction constant λ.

For example, when the first magnetic sublayer of the pinned magnetic layer is composed of Co_xFe_y ($y \geq 20$, $x+y=100$, and wherein each of x and y is represented as an atomic percent), the first magnetic sublayer has the bcc structure, an equivalent crystal plane represented by the {110} plane being preferentially oriented in the direction parallel to the boundary face. Since Co_xFe_y ($y \geq 20$, $x+y=100$) having the bcc structure has a magnetostriction constant λ larger than that of Co or Co_xFe_y ($20 \geq y$, $x+y=100$, and wherein each of x and y is represented as an atomic percent) having the fcc structure, this material allows a larger magnetoelastic effect to be achieved. Furthermore, the Co_xFe_y ($y \geq 20$, $x+y=100$) having the bcc structure has a large coercive force, and allows the magnetization of the pinned magnetic layer to be strongly pinned. However, when the iron content y of the Co_xFe_y is about 20 (atomic percent), this material may have a mixed structure including the fcc structure and the bcc structure.

Furthermore, according to the present invention, the first magnetic sublayer of the pinned magnetic layer preferably has a face-centered cubic (fcc) lattice structure in the vicinity of a boundary face adjacent to the nonmagnetic metal layer, an equivalent crystal plane represented by the {111} plane being preferentially oriented in the direction parallel to the boundary face; and the first magnetic sublayer of the pinned magnetic layer preferably has a body-centered cubic (bcc) lattice structure in the vicinity

of a boundary face adjacent to the nonmagnetic interlayer, an equivalent crystal plane represented by the {110} plane being preferentially oriented in the direction parallel to the boundary face.

When the vicinity of the boundary face of the first magnetic sublayer adjacent to the nonmagnetic interlayer has the bcc structure, the magnetostriction constant λ is increased, thereby achieving a larger magnetoelastic effect. On the other hand, when the vicinity of the boundary face of the first magnetic sublayer adjacent to the nonmagnetic metal layer has the fcc structure, the pinned magnetic layer, nonmagnetic conductive layer, and the free magnetic layer readily have a constant crystal orientation, thereby increasing the magnetoresistance ratio (MR ratio).

For example, the first magnetic sublayer of the pinned magnetic layer is preferably composed of Co_xFe_y ($20 \geq y$, $x+y=100$) or Co in the vicinity of the boundary face adjacent to the nonmagnetic metal layer; and the first magnetic sublayer of the pinned magnetic layer is preferably composed of Co_xFe_y ($y \geq 20$, $x+y=100$) in the vicinity of the boundary face adjacent to the nonmagnetic interlayer. In this case, the first magnetic sublayer of the pinned magnetic layer has the fcc structure in the vicinity of a boundary face adjacent to the nonmagnetic metal layer, an equivalent crystal plane represented by the {111} plane being preferentially oriented in the direction parallel to the boundary face; and the first magnetic sublayer of the pinned magnetic layer has the bcc structure in the vicinity of a boundary face adjacent to the

nonmagnetic interlayer, an equivalent crystal plane represented by the {110} plane being preferentially oriented in the direction parallel to the boundary face.

Furthermore, the first magnetic sublayer of the pinned magnetic layer is preferably composed of Co_xFe_y ($y \geq 20$, $x+y=100$) in the vicinity of the boundary face adjacent to the nonmagnetic interlayer because the Ruderman-Kittel-Kasuya-Yoshida (RKKY) interaction between the first magnetic sublayer and other magnetic sublayer via the nonmagnetic interlayer can be increased.

The iron content in the first magnetic sublayer of the pinned magnetic layer may gradually increases from the boundary face adjacent to the nonmagnetic metal layer to the boundary face adjacent to the nonmagnetic interlayer.

According to the present invention, in order to overlap the atoms in the nonmagnetic metal layer and the atoms in the first magnetic sublayer and to generate deformations in the crystal structure, a value calculated by dividing the difference between the nearest interatomic distance of the nonmagnetic metal layer in the plane parallel to the boundary face and the nearest interatomic distance of the first magnetic sublayer of the pinned magnetic layer in the plane parallel to the boundary face by the nearest interatomic distance of the first magnetic sublayer is preferably in the range of 0.05 to 0.20.

An interlayer is preferably disposed between the nonmagnetic metal layer and the first magnetic sublayer of the pinned magnetic layer, the interlayer being composed of

PtMn alloy or X-Mn alloy (wherein X is at least one element selected from the group consisting of Pd, Ir, Rh, Ru, Os, Ni, and Fe). In this case, the crystals in the nonmagnetic metal layer and the crystals in the interlayer are readily oriented in an epitaxial state, and the crystals in the interlayer and the crystals in the pinned magnetic layer are readily oriented in an epitaxial or a heteroepitaxial state.

The first magnetic sublayer may preferably be composed of a magnetic material having a positive magnetostriction constant.

Electrode layers composed of Cr, α-Ta, or Rh are preferably disposed at both sides of the free magnetic layer, the nonmagnetic conductive layer, and the pinned magnetic layer. In this case, the compressive stress in the track width direction (i.e., the tensile stress in the height direction) applied to the pinned magnetic layer can be increased.

The distance between the crystal planes of the electrode layers composed of Cr in the direction parallel to the layers is preferably 0.2044 nm (the distance between the {110} planes in the bcc structure) or more; the distance between the crystal planes of the electrode layers composed of α-Ta in the direction parallel to the layers is preferably 0.2337 nm (the distance between the {110} planes in the bcc structure) or more; or the distance between the crystal planes of the electrode layers composed of Rh in the direction parallel to the layers is preferably 0.2200 nm (the distance between the {111} planes in the fcc structure) or

more.

The magnetic sensor of the present invention is useful, in particular, in reduction in size. In particular, an optical track width of the pinned magnetic layer is preferably 0.15 μm or less.

According to the present invention described above in detail, in the magnetic sensor having the self-pinning type pinned magnetic layer, the mechanism to control the magnetostriction of the pinned magnetic layer is made clear, and the material of the nonmagnetic metal layer that is in contact with the pinned magnetic layer is appropriately selected. Thus, the present invention can provide a magnetic sensor that appropriately regulates the magnetostriction to strongly pin the magnetization of the pinned magnetic layer.

Embodiments of the invention will now be described, by way of example only, with reference to the accompanying drawings, in which:

Fig. 1 is a sectional view of a magnetic sensor according to a first embodiment of the present invention, viewed from a surface facing a recording medium;

Fig. 2 is a plan view of the magnetic sensor shown in Fig. 1;

Fig. 3 is a schematic view showing a nonmagnetic metal layer and a pinned magnetic layer are matched, while deformations are generated;

Fig. 4 is a schematic view showing the nonmagnetic metal layer and the pinned magnetic layer are matched;

Fig. 5 is a schematic view showing the nonmagnetic metal layer and the pinned magnetic layer are mismatched;

Fig. 6 is a partial sectional view in the vicinity of the pinned magnetic layer of the magnetic sensor according to the present invention;

Fig. 7 is a partial sectional view in the vicinity of the pinned magnetic layer of the magnetic sensor according to the present invention;

Fig. 8 is a partial sectional view in the vicinity of the pinned magnetic layer of the magnetic sensor according to the present invention;

Fig. 9 is a sectional view of a magnetic sensor according to a second embodiment of the present invention, viewed from a surface facing a recording medium;

Fig. 10 is a sectional view of a magnetic sensor according to a third embodiment of the present invention, viewed from a surface facing a recording medium;

Fig. 11 is a graph showing the magnetostriction of multilayer films formed by laminating the nonmagnetic metal layer and ferromagnetic sublayers; and

Fig. 12 is a sectional view of a known magnetic sensor, viewed from a surface facing a recording medium.

DESCRIPTION OF THE PREFERRED EMBODIMENTS

Fig. 1 is a sectional view of a magnetic sensor according to a first embodiment of the present invention, viewed from a surface facing a recording medium.

According to the magnetic sensor shown in Fig. 1, a multilayer film T1 is formed on a bottom gap layer 20 composed of an insulating material such as alumina.

According to the first embodiment shown in Fig. 1, the multilayer film T1 is formed by laminating, from the bottom, a seed layer 21, a nonmagnetic metal layer 22, a pinned magnetic layer 23, a nonmagnetic conductive layer 24, a free magnetic layer 25, and a protective layer 26 in that order.

The seed layer 21 is composed of, for example, NiFe alloy, NiFeCr alloy, Cr, or Ta. For example, the seed layer 21 is composed of $(Ni_{0.8}Fe_{0.2})_{60\ at\%}Cr_{40\ at\%}$, and has a thickness of 35 Å to 60 Å.

The seed layer 21 improves the {111} orientation of the nonmagnetic metal layer 22.

The nonmagnetic metal layer 22 will be described later.

The pinned magnetic layer 23 includes a first magnetic sublayer 23a, a second magnetic sublayer 23c, and a nonmagnetic interlayer 23b disposed therebetween. The pinned magnetic layer 23 has a synthetic ferrimagnetic structure. The magnetization of the pinned magnetic layer 23 is pinned in the height direction (in the Y direction in the figure) by means of the uniaxial anisotropy of the pinned magnetic layer 23 itself.

The nonmagnetic conductive layer 24 prevents a magnetic bond between the pinned magnetic layer 23 and the free magnetic layer 25. The nonmagnetic conductive layer 24 is preferably composed of a conductive nonmagnetic material such as Cu, Cr, Au, or Ag, and is, more preferably, composed of Cu. The nonmagnetic conductive layer 24 has a thickness of 17 Å to 30 Å.

The free magnetic layer 25 is composed of a magnetic

material such as NiFe alloy or CoFe alloy. According to the first embodiment shown in Fig. 1, when the free magnetic layer 25 is composed of, in particular, NiFe alloy, a diffusion barrier layer (not shown in the figure) composed of, for example, Co or CoFe, is preferably formed between the free magnetic layer 25 and the nonmagnetic conductive layer 24. The free magnetic layer 25 has a thickness of 20 Å to 60 Å. The free magnetic layer 25 may have a synthetic ferrimagnetic structure in which a plurality of magnetic sublayers is laminated with a nonmagnetic interlayer therebetween.

The protective layer 26, which is composed of, for example, Ta, suppresses oxidation of the multilayer film T1. The protective layer 26 has a thickness of 10 Å to 50 Å.

According to the first embodiment shown in Fig. 1, at both sides of the multilayer film T1 that includes from the seed layer 21 to the protective layer 26, bias base layers 27, hard bias layers 28, and electrode layers 29 are formed. The magnetization of the free magnetic layer 25 is aligned in the track width direction (in the X direction in the figure) by a longitudinal bias magnetic field from the hard bias layers 28.

The bias base layers 27 are composed of Cr, W, or Ti. The hard bias layers 28 are composed of, for example, Co-Pt (cobalt-platinum) alloy or Co-Cr-Pt (cobalt-chromium-platinum) alloy. The electrode layers 29 are composed of, for example, Cr, Ta, Rh, Au, or W (tungsten).

The bias base layers 27 have a thickness of 20 Å to 100 Å. The hard bias layers 28 have a thickness of 100 Å to 400

Å. The electrode layers 29 have a thickness of 400 Å to 1,500 Å.

A top gap layer 30 composed of an insulating material such as alumina is formed on the electrode layers 29 and the protective layer 26. Although not shown in the figure, a bottom shield layer is formed under the bottom gap layer 20 and a top shield layer is formed on the top gap layer 30. The bottom shield layer and the top shield layer are composed of a soft magnetic material such as NiFe. Each of the top gap layer 30 and the bottom gap layer 20 has a thickness of 50 Å to 300 Å.

The magnetization of the free magnetic layer 25 is aligned in the track width direction (in the X direction in the figure) by a longitudinal bias magnetic field from the hard bias layers 28. The magnetization of the free magnetic layer 25 is sensitively changed in response to a signal magnetic field (an external magnetic field) generated from the recording medium. On the other hand, the magnetization of the pinned magnetic layer 23 is pinned in the height direction (in the Y direction in the figure).

The relationship between the changes of magnetization direction of the free magnetic layer 25 and the pinned magnetization direction of the pinned magnetic layer 23 (in particular, the pinned magnetization direction of the second magnetic sublayer 23c) changes the electrical resistance. A leakage field from the recording medium is detected by changes of voltage or current based on the change of the electrical resistance.

The features of the present embodiment will now be described.

The pinned magnetic layer 23 of the magnetic sensor shown in Fig. 1 includes a first magnetic sublayer 23a, a second magnetic sublayer 23c, and a nonmagnetic interlayer 23b disposed therebetween. The pinned magnetic layer 23 has the synthetic ferrimagnetic structure. The magnetization of the first magnetic sublayer 23a and the magnetization of the second magnetic sublayer 23c are aligned in antiparallel directions with respect to each other by the Ruderman-Kittel-Kasuya-Yoshida (RKKY) interaction via the nonmagnetic interlayer 23b.

The distance from the first magnetic sublayer 23a to the nonmagnetic conductive layer 24 is larger than the distance from the second magnetic sublayer 23c to the nonmagnetic conductive layer 24. The first magnetic sublayer 23a is in contact with the nonmagnetic metal layer 22.

The nonmagnetic metal layer 22 is composed of at least one element selected from the group consisting of Ru, Re, Os, Ti, Rh, Ir, Pd, Pt, and Al. The nonmagnetic metal layer 22 has a thickness of 5 Å to 30 Å.

The magnetic sensor shown in Fig. 1 does not have an antiferromagnetic layer that is overlapped with the pinned magnetic layer 23. According to this magnetic sensor, the magnetization of the pinned magnetic layer 23 is pinned by means of the uniaxial anisotropy of the pinned magnetic layer 23 itself, that is, the magnetic sensor is a self-pinning type magnetic sensor.

Accordingly, the shunt loss can be small compared with a magnetic sensor having the antiferromagnetic layer. Thus, the output in detecting the magnetic field of the magnetic sensor can be improved by 20% to 30%. Furthermore, the distance between the top shield layer and the bottom shield layer, which are disposed on and under the magnetic sensor, respectively, can be small, thereby achieving a higher linear recording density on the recording medium.

According to the first embodiment, the second magnetic sublayer 23c has a thickness larger than the thickness of the first magnetic sublayer 23a. The magnetization direction of the second magnetic sublayer 23c is pinned in the height direction (in the Y direction in the figure), and the magnetization direction of the first magnetic sublayer 23a is pinned in the direction antiparallel to the height direction.

The first magnetic sublayer 23a has a thickness of 10 Å to 30 Å, and the second magnetic sublayer 23c has a thickness of 15 Å to 35 Å. A large thickness of the first magnetic sublayer 23a increases the coercive force. However, a large thickness of the first magnetic sublayer 23a increases the shunt loss. As described later, the first magnetic sublayer 23a is matched with the nonmagnetic metal layer 22, thereby generating deformations in the crystal structure. The deformations increase the magnetostriction constant λ and the uniaxial anisotropy. However, too large a thickness of the first magnetic sublayer 23a decreases the deformations generated in the first magnetic sublayer 23a, thereby decreasing the magnetostriction constant λ and the uniaxial

anisotropy.

The uniaxial anisotropy to pin the magnetization of the pinned magnetic layer 23 is determined by an induced magnetic anisotropy and a magnetoelastic effect. The present invention mainly utilizes the magnetoelastic effect.

The magnetoelastic effect is controlled by the magnetoelastic energy. The magnetoelastic energy is defined by the stress σ on the pinned magnetic layer 23 and the magnetostriction constant λ of the pinned magnetic layer 23.

Fig. 2 is a plan view of the magnetic sensor shown in Fig. 1, viewed from the upper side in the figure (the direction opposite to the Z direction in the figure). The multilayer film T1 of the magnetic sensor is formed between a pair of bias base layers 27, hard bias layers 28, and electrode layers 29. Fig. 2 does not show the bias base layers 27 and the hard bias layers 28, because these layers are disposed under the electrode layers 29. An insulating layer 31, shown by diagonal lines, fills the space around the multilayer film T1, the bias base layers 27, the hard bias layers 28, and the electrode layers 29.

An end face F of the multilayer film T1, the bias base layers 27, the hard bias layers 28, and the electrode layers 29, the end face F opposing a face of the recording medium, is exposed or just covered with a thin protective layer. The thin protective layer is composed of, for example, diamond like carbon (DLC), and has a thickness of 20 Å to 50 Å. That is, the end face F is an open end.

Accordingly, the stresses from the bottom gap layer 20

and the top gap layer 30, both of which were originally isotropic two-dimensionally, is relieved at the end face F. As a result, the symmetry is lost, and a tensile stress is applied to the multilayer film T1 in the direction parallel to the height direction (the Y direction in the figure). When the laminated films composed of the bias base layers 27, the hard bias layers 28, and the electrode layers 29 have a compressible internal stress, the layers such as the electrode layers try to extend in the longitudinal directions. Accordingly, a compressive stress is applied to the multilayer film T1 in the parallel direction and the antiparallel direction with respect to the track width direction (the X direction in the figure).

That is, the tensile stress in the height direction and the compressive stress in the track width direction are applied to the pinned magnetic layer 23, of which the end face F opposing the face of the recording medium is opened. The first magnetic sublayer 23a is composed of a magnetic material having a positive magnetostriction constant. Accordingly, the easy magnetization axis of the first magnetic sublayer 23a is parallel to the inner part of the magnetic sensor (the height direction, or the Y direction in the figure) due to the magnetoelastic effect. The magnetization direction of the first magnetic sublayer 23a is pinned in the direction parallel to the height direction or antiparallel to the height direction. The magnetization of the second magnetic sublayer 23c is pinned in the direction antiparallel to the magnetization direction of the first

magnetic sublayer 23a by the RKKY interaction via the nonmagnetic interlayer 23b.

According to the present invention, the increase of the magnetostriction constant of the pinned magnetic layer 23 increases the magnetoelastic energy, thereby increasing the uniaxial anisotropy of the pinned magnetic layer 23. The increase of uniaxial anisotropy of the pinned magnetic layer 23 allows the magnetization of the pinned magnetic layer 23 to be strongly pinned in one direction. Furthermore, the increase of uniaxial anisotropy of the pinned magnetic layer 23 increases the output of the magnetic sensor and improves the output stability and the symmetry.

Specifically, the first magnetic sublayer 23a of the pinned magnetic layer 23 is bonded with the nonmagnetic metal layer 22 to generate deformations in the crystal structure of the first magnetic sublayer 23a. Thus, the magnetostriction constant λ of the first magnetic sublayer 23a is increased. The nonmagnetic metal layer 22 is composed of at least one element selected from the group consisting of Ru, Re, Os, Ti, Rh, Ir, Pd, Pt, and Al.

When the nonmagnetic metal layer 22 is composed of at least one element selected from the group consisting of Rh, Ir, Pd, Pt, and Al, the nonmagnetic metal layer 22 has a face-centered cubic (fcc) structure. In this case, an equivalent crystal plane represented by a {111} plane is preferentially oriented in the direction parallel to the boundary face. When the nonmagnetic metal layer 22 is composed of at least one element selected from the group

consisting of Ru, Re, Os, and Ti, the nonmagnetic metal layer 22 has a hexagonal close-packed (hcp) structure. In this case, a C-plane ({0001} plane) is preferentially oriented in the direction parallel to the boundary face.

On the other hand, when the first magnetic sublayer 23a of the pinned magnetic layer 23 is composed of Co or Co_xFe_y ($20 \geq y$, $x+y=100$), the first magnetic sublayer 23a has a face-centered cubic (fcc) lattice structure. In the first magnetic sublayer 23a, an equivalent crystal plane represented by the {111} plane is preferentially oriented in the direction parallel to the boundary face.

Accordingly, the atoms in the first magnetic sublayer 23a and the atoms in the nonmagnetic metal layer 22 are readily overlapped with each other, and the crystals in the nonmagnetic metal layer 22 and the crystals in the pinned magnetic layer 23 are oriented in an epitaxial state.

However, a certain amount of difference is required between the nearest interatomic distance in the {111} plane of the first magnetic sublayer 23a and the nearest interatomic distance in the {111} plane or in the C-plane of the nonmagnetic metal layer 22.

According to the first embodiment, in order to overlap the atoms in the nonmagnetic metal layer 22 and the atoms in the first magnetic sublayer 23a, and to generate deformations in the crystal structure, a value (hereinafter referred to as mismatch value) is controlled in the range of 0.05 to 0.20. The mismatch value is defined as follows: the difference between the nearest interatomic distance in the {111} plane

or in the C-plane of the nonmagnetic metal layer 22 and the nearest interatomic distance in the {111} plane of the first magnetic sublayer 23a of the pinned magnetic layer 23 is divided by the nearest interatomic distance in the {111} plane of the first magnetic sublayer 23a.

Table 1 shows lattice constants of crystals having the fcc structure, the nearest interatomic distances in the {111} plane of the crystals having the fcc structure, and the mismatch percentage (mismatch %) of the crystals having the fcc structure with Co having the fcc structure. The mismatch percentage is calculated by multiplying the mismatch value by 100, and is represented as a percentage.

Table 2 shows the nearest interatomic distances (that correspond to the lattice constants a) in the C-plane of crystals having the hcp structure and the mismatch percentage of the crystals having the hcp structure with Co having the fcc structure.

Table 1

Material	Lattice Constant (Å)	Nearest Interatomic Distance	Mismatch Percentage with Co (%)
Co (fcc)	3.545	2.506	
Ph	3.803	2.689	7.290
Pd	3.890	2.751	9.736
Ir	3.839	2.715	8.314
Pt	3.923	2.774	10.675
Al	4.049	2.863	14.238
Below: Comparative Examples			
$(Ni_{0.8}Fe_{0.2})_{60}Cr_{40}$	3.568	2.523	0.657
Cu	3.615	2.556	1.995
$Ni_{80}Fe_{20}$	3.549	2.509	0.120
Si	5.430	3.840	53.189
Ge	5.658	4.001	59.607
Pb	4.951	3.501	39.662

Table 2

Material	Lattice Constant a (Å)	Mismatch Percentage with Co (%)
Ru	2.706	7.952
Ti	2.950	17.695
Re	2.760	10.115
Os	2.734	9.081
Below: Comparative Examples		
Hf	3.197	27.537
Zr	3.232	28.946

Referring to Table 1, the mismatch percentage with Co having the fcc structure in Rh crystal, Ir crystal, Pd crystal, Pt crystal, and Al crystal is in the range of 7% to 14% (i.e., the mismatch value is in the range of 0.07 to 0.14). Referring to Table 2, the mismatch percentage with Co having the fcc structure in Ru crystal, Re crystal, Os crystal, and Ti crystal is in the range of 7% to 18% (i.e., the mismatch value is in the range of 0.07 to 0.18).

As schematically shown in Fig. 3, when the mismatch percentage between the nonmagnetic metal layer 22 and the first magnetic sublayer 23a, both of which are overlapped, is from 5% to 20% (or the mismatch value is from 0.05 to 0.20), the atoms in the nonmagnetic metal layer 22 and the atoms in the first magnetic sublayer 23a are overlapped, while the crystal structure is deformed in the vicinity of the boundary

face.

In Fig. 3, a symbol N1 indicates the nearest interatomic distance in the {111} plane of the first magnetic sublayer 23a, and a symbol N2 indicates the nearest interatomic distance in the {111} plane or in the C-plane of the nonmagnetic metal layer 22. The values of N1 and N2 are measured at remote places from the boundary face between the nonmagnetic metal layer 22 and the first magnetic sublayer 23a, those places barely being affected by the deformations.

Thus, the generation of deformations in the crystal structure of the first magnetic sublayer 23a increases the magnetostriction constant λ of the first magnetic sublayer 23a, thereby increasing the magnetoelastic effect.

If the nonmagnetic metal layer 22 is composed of $(Ni_{0.8}Fe_{0.2})_{60}Cr_{40}$, Cu, or, $Ni_{80}Fe_{20}$, and the first magnetic sublayer 23a is composed of Co, the mismatch percentage between the nonmagnetic metal layer 22 and the first magnetic sublayer 23a is too small. That is, as schematically shown in Fig. 4, when the atoms in the nonmagnetic metal layer 22 and the atoms in the first magnetic sublayer 23a are overlapped, deformations of the crystal structure in the vicinity of the boundary face does not occur. Accordingly, the magnetostriction constant λ of the first magnetic sublayer 23a cannot be increased.

If the nonmagnetic metal layer 22 is composed of Si, Ge, Pb, Hf, or Zr, and the first magnetic sublayer 23a is composed of Co, the mismatch percentage between the nonmagnetic metal layer 22 and the first magnetic sublayer

23a is too large. That is, as schematically shown in Fig. 5, the atoms in the nonmagnetic metal layer 22 and the atoms in the first magnetic sublayer 23a are not overlapped, and are mismatched or are in a non-epitaxial state. When the atoms in the nonmagnetic metal layer 22 and the atoms in the first magnetic sublayer 23a are in a non-epitaxial state, deformations of the crystal structure in the vicinity of the boundary face does not occur. Accordingly, the magnetostriction constant λ of the first magnetic sublayer 23a cannot be increased.

The first magnetic sublayer 23a of the pinned magnetic layer 23 may have a body-centered cubic (bcc) lattice structure. In the first magnetic sublayer 23a, an equivalent crystal plane represented by a {110} plane may be preferentially oriented in the direction parallel to the boundary face.

For example, when the first magnetic sublayer 23a of the pinned magnetic layer 23 is composed of Co_xFe_y ($y \geq 20$, $x+y=100$), the first magnetic sublayer 23a has the body-centered cubic (bcc) lattice structure.

As described above, the nonmagnetic metal layer 22 is composed of at least one element selected from the group consisting of Rh, Ir, Pd, Pt, Al, Ru, Re, Os, and Ti. The nonmagnetic metal layer 22 may have the fcc structure, and in this case, the equivalent crystal plane represented by the {111} plane is preferentially oriented in the direction parallel to the boundary face. Alternatively the nonmagnetic metal layer 22 may have the hcp structure, and in this case,

the C-plane is preferentially oriented in the direction parallel to the boundary face.

The atomic arrangement in the equivalent crystal plane represented by the {110} plane of the crystal having the bcc structure is similar to the atomic arrangement in the equivalent crystal plane represented by the {111} plane of the crystal having the fcc structure. Therefore, the crystal having the bcc structure and the crystal having the fcc structure can be matched, that is, the atoms can be overlapped and can be oriented in a heteroepitaxial state.

The atomic arrangement in the equivalent crystal plane represented by the {110} plane of the crystal having the bcc structure is similar to the atomic arrangement in the C-plane of the crystal having the hcp structure. Therefore, the crystal having the bcc structure and the crystal having the hcp structure can be matched, that is, the atoms can be overlapped and can be oriented in a heteroepitaxial state.

Accordingly, the atoms in the first magnetic sublayer 23a and the atoms in the nonmagnetic metal layer 22 are readily overlapped with each other, and the crystals in the nonmagnetic metal layer 22 and the crystals in the first magnetic sublayer 23a of the pinned magnetic layer 23 are oriented in a heteroepitaxial state.

There is a certain amount of difference between the nearest interatomic distance in the {110} plane of the first magnetic sublayer 23a and the nearest interatomic distance in the {111} plane or in the C-plane of the nonmagnetic metal layer 22. Accordingly, in the vicinity of the boundary face

between the first magnetic sublayer 23a and the nonmagnetic metal layer 22, the atoms in the first magnetic sublayer 23a and the atoms in the nonmagnetic metal layer 22 are overlapped with each other, while each of the crystal structures is deformed. Thus, the generation of the deformations in the crystal structure of the first magnetic sublayer 23a can increase the magnetostriction constant λ.

Since Co_xFe_y ($y \geq 20$, $x+y=100$) having the bcc structure has a magnetostriction constant λ larger than that of Co or Co_xFe_y ($20 \geq y$, $x+y=100$), both of which have the fcc structure, in particular in about y=50 (atomic percent), this material allows a larger magnetoelastic effect to be achieved. Furthermore, the Co_xFe_y ($y \geq 20$, $x+y=100$) having the bcc structure has a large coercive force, and allows the magnetization of the pinned magnetic layer 23 to be strongly pinned.

According to the present invention, it is sufficient that most of the atoms in the first magnetic sublayer 23a and in the nonmagnetic metal layer 22 are matched, that is, most of the atoms be overlapped with each other, in the vicinity of the boundary face between the first magnetic sublayer 23a and the nonmagnetic metal layer 22. For example, as schematically shown in Fig. 3, the boundary area may partly have regions in which the atoms in the first magnetic sublayer 23a and the atoms in the nonmagnetic metal layer 22 are not overlapped.

The second magnetic sublayer 23c may be composed of either Co_xFe_y ($y \geq 20$, $x+y=100$), which has the bcc structure,

or Co or Co_xFe_y ($20 \geq y$, $x+y=100$), both of which have the fcc structure.

The use of Co_xFe_y ($y \geq 20$, $x+y=100$) having the bcc structure as the second magnetic sublayer 23c increases the positive magnetostriction. The Co_xFe_y ($y \geq 20$, $x+y=100$) having the bcc structure has a large coercive force, and allows the magnetization of the pinned magnetic layer 23 to be strongly pinned. Furthermore, the RKKY interaction between the first magnetic sublayer 23a and the second magnetic sublayer 23c via the nonmagnetic interlayer 23b can be increased.

On the other hand, the second magnetic sublayer 23c is in contact with the nonmagnetic conductive layer 24, and greatly affects the magnetoresistive effect. The use of Co or Co_xFe_y ($20 \geq y$, $x+y=100$) having the fcc structure decreases the deterioration of the magnetoresistive effect.

Figs. 6 to 8 are partial sectional views showing other embodiments of the pinned magnetic layer 23.

Referring to Fig. 6, the first magnetic sublayer 23a in the pinned magnetic layer 23 may include an fcc magnetic sublayer 23a1 adjacent to the nonmagnetic metal layer 22, and a bcc magnetic sublayer 23a2 adjacent to the nonmagnetic interlayer 23b.

The fcc magnetic sublayer 23a1 has the face-centered cubic (fcc) lattice structure, and the equivalent crystal plane represented by the {111} plane is preferentially oriented in the direction parallel to the boundary face. The bcc magnetic sublayer 23a2 has the body-centered cubic (bcc) lattice structure, and the equivalent crystal plane

represented by the {110} plane is preferentially oriented in the direction parallel to the boundary face.

The fcc magnetic sublayer 23a1 is composed of Co or Co_xFe_y ($20 \geq y$, $x+y=100$), and the bcc magnetic sublayer 23a2 is composed of Co_xFe_y ($y \geq 20$, $x+y=100$).

In the vicinity of the boundary face of the first magnetic sublayer 23a adjacent to the nonmagnetic interlayer 23b, the first magnetic sublayer 23a has the bcc structure, thereby increasing the magnetostriction constant λ and achieving a large magnetoelastic effect. When the first magnetic sublayer 23a adjacent to the nonmagnetic interlayer 23b is composed of Co_xFe_y ($y \geq 20$, $x+y=100$), the RKKY interaction between the first magnetic sublayer 23a and the second magnetic sublayer 23c via the nonmagnetic interlayer 23b is increased.

On the other hand, in the vicinity of the boundary face of the first magnetic sublayer 23a adjacent to the nonmagnetic metal layer 22, the first magnetic sublayer 23a has the fcc structure. In this case, the pinned magnetic layer 23, the nonmagnetic conductive layer 24, and the free magnetic layer 25 have a constant crystal orientation, and have large crystal grains, thereby increasing the magnetoresistance ratio (MR ratio).

Referring to Fig. 7, the second magnetic sublayer 23c in the pinned magnetic layer 23 may include an fcc magnetic sublayer 23c2 adjacent to the nonmagnetic conductive layer 24, and a bcc magnetic sublayer 23c1 adjacent to the nonmagnetic interlayer 23b.

The fcc magnetic sublayer 23c2 has the face-centered cubic (fcc) lattice structure, and the equivalent crystal plane represented by the {111} plane is preferentially oriented in the direction parallel to the boundary face. The bcc magnetic sublayer 23c1 has the body-centered cubic (bcc) lattice structure, and the equivalent crystal plane represented by the {110} plane is preferentially oriented in the direction parallel to the boundary face.

The fcc magnetic sublayer 23c2 is composed of Co or Co_xFe_y ($20 \geq y$, $x+y=100$), and the bcc magnetic sublayer 23c1 is composed of Co_xFe_y ($y \geq 20$, $x+y=100$).

In the vicinity of the boundary face of the second magnetic sublayer 23c adjacent to the nonmagnetic interlayer 23b, the second magnetic sublayer 23c has the bcc structure, thereby increasing the magnetostriction constant λ and achieving a large magnetoelastic effect. When the second magnetic sublayer 23c adjacent to the nonmagnetic interlayer 23b is composed of Co_xFe_y ($y \geq 20$, $x+y=100$), the RKKY interaction between the first magnetic sublayer 23a and the second magnetic sublayer 23c via the nonmagnetic interlayer 23b is increased.

On the other hand, in the vicinity of the boundary face of the second magnetic sublayer 23c adjacent to the nonmagnetic conductive layer 24, the second magnetic sublayer 23c has the fcc structure, thereby suppressing the deterioration of the magnetoresistive effect.

Referring to Fig. 8, the first magnetic sublayer 23a in the pinned magnetic layer 23 may include the fcc magnetic

sublayer 23a1 adjacent to the nonmagnetic metal layer 22, and the bcc magnetic sublayer 23a2 adjacent to the nonmagnetic interlayer 23b. In addition, the second magnetic sublayer 23c may include the fcc magnetic sublayer 23c2 adjacent to the nonmagnetic conductive layer 24, and the bcc magnetic sublayer 23c1 adjacent to the nonmagnetic interlayer 23b.

Referring to Figs. 6 to 8, the fcc magnetic sublayer 23a1 and the bcc magnetic sublayer 23a2 are laminated to form the first magnetic sublayer 23a, and/or the bcc magnetic sublayer 23c1 and the fcc magnetic sublayer 23c2 are laminated to form the second magnetic sublayer 23c.

However, according to the present invention, it is sufficient that in the vicinity of the boundary face of the first magnetic sublayer 23a of the pinned magnetic layer 23 adjacent to the nonmagnetic metal layer 22, the first magnetic sublayer 23a has the face-centered cubic (fcc) lattice structure, and the equivalent crystal plane represented by the {111} plane is preferentially oriented in the direction parallel to the boundary face. Also, it is sufficient that in the vicinity of the boundary face of the first magnetic sublayer 23a adjacent to the nonmagnetic interlayer 23b, the first magnetic sublayer 23a has the body-centered cubic (bcc) lattice structure, and the equivalent crystal plane represented by the {110} plane is preferentially oriented in the direction parallel to the boundary face.

Accordingly, the first magnetic sublayer 23a of the pinned magnetic layer 23 may have the following structure.

In the vicinity of the boundary face of the first magnetic sublayer 23a of the pinned magnetic layer 23 adjacent to the nonmagnetic metal layer 22, the first magnetic sublayer 23a may be composed of Co or Co_xFe_y ($20 \geq y$, $x+y=100$), and has the fcc structure, and the equivalent crystal plane represented by the {111} plane may be preferentially oriented in the direction parallel to the boundary face. Furthermore, the iron content in the first magnetic sublayer 23a may gradually increase from the vicinity of the boundary face adjacent to the nonmagnetic metal layer 22 to another boundary face adjacent to the nonmagnetic interlayer 23b. Furthermore, in the vicinity of the boundary face of the first magnetic sublayer 23a adjacent to the nonmagnetic interlayer 23b, the first magnetic sublayer 23a may be composed of Co_xFe_y ($y \geq 20$, $x+y=100$), and has the body-centered cubic (bcc) lattice structure, and the equivalent crystal plane represented by the {110} plane may be preferentially oriented in the direction parallel to the boundary face.

The second magnetic sublayer 23c may also be composed of a CoFe alloy in which the iron content gradually increases from the vicinity of the boundary face adjacent to the nonmagnetic conductive layer 24 to another boundary face adjacent to the nonmagnetic interlayer 23b.

Fig. 9 is a sectional view of a magnetic sensor according to a second embodiment of the present invention, viewed from a surface facing a recording medium.

The difference between magnetic sensors shown in Fig. 9 and Fig. 1 is that the magnetic sensor shown in Fig. 9

further includes an interlayer 40. The interlayer 40 is disposed between the nonmagnetic metal layer 22 and the first magnetic sublayer 23a of the pinned magnetic layer 23, and is composed of PtMn alloy or X-Mn alloy (wherein X is at least one element selected from the group consisting of Pd, Ir, Rh, Ru, Os, Ni, and Fe).

According to the second embodiment, the interlayer 40 has a thickness of 5 Å to 50 Å. When the interlayer 40 composed of PtMn alloy or X-Mn alloy (wherein X is at least one element selected from the group consisting of Pd, Ir, Rh, Ru, Os, Ni, and Fe) has a thickness in this range, the crystal structure of the interlayer 40 maintains the face-centered cubic (fcc) structure formed when depositing the layer.

Accordingly, the atoms in the interlayer 40 and the atoms in the first magnetic sublayer 23a of the pinned magnetic layer 23 are readily overlapped with each other. Thus, the crystals in the interlayer 40 and the crystals in the first magnetic sublayer 23a are readily matched to be epitaxial or heteroepitaxial.

There is a certain amount of difference between the nearest interatomic distance in the {111} plane or the {110} plane of the first magnetic sublayer 23a and the nearest interatomic distance in the {111} plane of the interlayer 40. Accordingly, in the vicinity of the boundary face between the first magnetic sublayer 23a and the interlayer 40, the atoms in the first magnetic sublayer 23a and the atoms in the interlayer 40 are overlapped with each other, while each of

the crystal structures is deformed. Thus, the generation of the deformations in the crystal structure of the first magnetic sublayer 23a can increase the magnetostriction constant λ. Furthermore, the crystals in the nonmagnetic metal layer 22 and the crystals in the interlayer 40 are also readily oriented in an epitaxial state.

Furthermore, the nearest interatomic distance in the {111} plane of the interlayer 40 composed of PtMn alloy or X-Mn alloy (wherein X is at least one element selected from the group consisting of Pd, Ir, Rh, Ru, Os, Ni, and Fe) is controlled to be larger than the nearest interatomic distance in the {111} plane or in the C-plane of the nonmagnetic metal layer 22. Thus, the nearest interatomic distance in the direction parallel to the layer can be gradually increased from the seed layer 21 to the interlayer 40, thereby suppressing an excessive deformation in the multilayer film T1.

The interlayer 40 having a thickness of more than 50 Å is not preferable, because the crystal structure of the interlayer 40 is transformed into a face-centered tetragonal (fct) structure (CuAu-I type ordered structure) at 250°C or higher. However, even if the interlayer 40 has a thickness of more than 50 Å, the crystal structure of the interlayer 40 maintains the face-centered cubic (fcc) structure being formed when depositing the layer, at lower than 250°C.

Fig. 10 is a sectional view of a magnetic sensor according to a third embodiment of the present invention, viewed from a surface facing a recording medium.

Although the magnetic sensor shown in Fig. 10 is similar to the magnetic sensor shown in Fig. 9, the magnetic sensor shown in Fig. 10 includes a multilayer film T2 instead of the multilayer film T1 in Fig. 9. The multilayer film T2 is formed by laminating, from the bottom, the seed layer 21; the free magnetic layer 25; the nonmagnetic conductive layer 24; the pinned magnetic layer 23 composed of the second magnetic sublayer 23c, the nonmagnetic interlayer 23b, and the first magnetic sublayer 23a; the interlayer 40; the nonmagnetic metal layer 22; and the protective layer 26. In other words, the laminating order in the multilayer film T2 is opposite to that in the multilayer film T1.

According to the magnetic sensor of the third embodiment, the first magnetic sublayer 23a of the pinned magnetic layer 23 is also in contact with the interlayer 40.

According to the third embodiment, the interlayer 40 also has a thickness of 5 Å to 50 Å. The crystal structure of the interlayer 40 also maintains the face-centered cubic (fcc) structure being formed when depositing the layer.

Accordingly, the atoms in the interlayer 40 and the atoms in the first magnetic sublayer 23a of the pinned magnetic layer 23 are readily overlapped with each other. Thus, the crystals in the interlayer 40 and the crystals in the first magnetic sublayer 23a are readily matched to be epitaxial.

Furthermore, there is a certain amount of difference between the nearest interatomic distance in the {111} plane or the {110} plane of the first magnetic sublayer 23a and the

nearest interatomic distance in the {111} plane of the interlayer 40. Accordingly, in the vicinity of the boundary face between the first magnetic sublayer 23a and the interlayer 40, the atoms in the first magnetic sublayer 23a and the atoms in the interlayer 40 are overlapped with each other, while each of the crystal structures is deformed. Thus, the generation of the deformations in the crystal structure of the first magnetic sublayer 23a can increase the magnetostriction constant λ. Furthermore, the crystals in the nonmagnetic metal layer 22 and the crystals in the interlayer 40 are also readily in an epitaxial state, thus suppressing an excessive deformation in the multilayer film T2, as in the magnetic sensor shown in Fig. 9. The nearest interatomic distances in the plane may be arranged stepwise as follows: "the nearest interatomic distance in the plane of the nonmagnetic metal layer 22">"the nearest interatomic distance in the plane of the interlayer 40">"the nearest interatomic distance in the plane of the first magnetic sublayer 23a". In this case, the matching at the boundary face can be maintained, while a larger lattice deformation can be applied to the first magnetic sublayer 23a.

Even if the interlayer 40 is not formed and the nonmagnetic metal layer 22 is directly in contact with the first magnetic sublayer 23a of the pinned magnetic layer 23, the atoms in the first magnetic sublayer 23a and the atoms in the nonmagnetic metal layer 22 are overlapped with each other, while each of the crystal structures is deformed. Thus, the magnetostriction constant λ of the first magnetic sublayer

23a can be increased.

In order to increase the anisotropy due to the magnetoelastic effect of the pinned magnetic layer 23, the compressive stress to the multilayer film T1 or T2 from the bias base layers 27, the hard bias layers 28, and the electrode layers 29, in the direction parallel and antiparallel to the track width direction (the X direction in the figure) is preferably increased.

For example, the compressive stress to the multilayer film T1 or T2 can be increased in the following cases: The electrode layers 29 are composed of Cr (chromium), α-Ta, or Rh. Furthermore, in the electrode layers 29 composed of Cr, the distance between the crystal planes of the electrode layers 29 in the direction parallel to the layers is 0.2044 nm (the distance between the {110} planes in the bcc structure) or more. In the electrode layers 29 composed of α-Ta, the distance is 0.2337 nm (the distance between the {110} planes in the bcc structure) or more. In the electrode layers 29 composed of Rh, the distance is 0.2200 nm (the distance between the {111} planes in the fcc structure) or more. In those cases, the compressive stress is applied in the directions indicated by arrows shown in Fig. 2. That is, the compressive stress is applied such that the electrode layers 29 are expanded towards the outside. Furthermore, the compressive stress is applied to the multilayer film T1 or T2 in the direction parallel and antiparallel to the track width direction (the X direction in the figure).

The distance between the crystal planes of the electrode

layers 29 in the direction parallel to the layers can be measured by X-ray diffractometry or electron diffractometry. In a layer composed of pure Cr, the distance between the crystal planes in the direction parallel to the layers is 0.2040 nm (the distance between the {110} planes in the bcc structure). In a layer composed of pure α-Ta, the distance is 0.2332 nm (the distance between the {110} planes in the bcc structure). In a layer composed of pure Rh, the distance is 0.2196 nm (the distance between the {111} planes in the fcc structure). When the distances between the crystal planes are equal to or larger than the above values, the electrode layers 29 give compressive stress to the multilayer film T1.

If the material of the electrode layers 29 is different, i.e., Cr or a soft metal such as Au, the above compressive stress is different, as follows.

For example, laminated films composed of, from the bottom, bias base layer: Cr (50 Å)/ hard bias layer: CoPt (200 Å)/ interlayer: Ta (50 Å)/ electrode layer: Au (800 Å)/ protective layer: Ta (50 Å), generate a compressive stress of 280 MPa.

On the other hand, laminated films composed of, from the bottom, bias base layer: Cr (50 Å)/ hard bias layer: CoPt (200 Å)/ interlayer: Ta (50 Å)/ electrode layer: Cr (1,400 Å)/ protective layer: Ta (50 Å), generate a compressive stress of 670 MPa.

Although the interlayer composed of Ta (50 Å) and the protective layer composed of Ta (50 Å) are not shown in Fig.

1, the interlayer functions as a layer to adjust the orientation of the electrode layers, and the protective layer functions as a layer to prevent oxidation.

The electrode layers 29 are deposited by ion beam sputtering. The pressure of gases such as Ar, Xe, and Kr in the sputtering apparatus is as low as 5×10^{-3} to 1×10^{-1} (Pa). A low pressure of the gases such as Ar, Xe, and Kr in the sputtering apparatus decreases the probability of Cr, α-Ta, or Ph atoms for forming the electrode layers colliding with Ar atoms. Therefore, the atoms such as Cr atoms are deposited while maintaining a high energy. When, for example, Cr atoms coming from the target and having a high energy collide with and are embedded on a film composed of, for example, Cr that has already been deposited, the electrode layers 29 are expanded toward the outside.

The longitudinal bias magnetic field generated from the hard bias layers 28 readily tilts the magnetization direction at both ends of the pinned magnetic layer 23 in the track width direction. However, a large compressive stress is applied to both ends of the pinned magnetic layer 23 in the track width direction. Accordingly, the anisotropy due to the magnetoelastic effect is increased at both ends of the pinned magnetic layer 23 in the track width direction, and thus, the magnetization direction can be strongly pinned in one direction.

According to the present invention, the magnetization direction of the pinned magnetic layer 23 is pinned by means of the uniaxial anisotropy based on the relationship between

the compressive stress from both sides of the pinned magnetic layer 23 and the magnetostriction. The compressive stress at the pinned magnetic layer is large at both ends of the pinned magnetic layer 23 in the optical track width direction, and is small at the center. Accordingly, a large width of the pinned magnetic layer 23 in the optical track width direction decreases the fixing power in the magnetization direction at the center of the pinned magnetic layer 23. Therefore, an optical track width W1 of the pinned magnetic layer 23 is preferably 0.15 μm or less.

The free magnetic layer 25 preferably has a negative magnetostriction. As described above, a compressive stress is applied to the multilayer film T1 of the magnetic sensor from both sides of the multilayer film T1. Accordingly, in the free magnetic layer 25 having a negative magnetostriction, the direction parallel or antiparallel to the track width direction (the X direction in the figure) readily becomes the easy magnetization axis due to the magnetoelastic effect.

Because of a demagnetizing field, the magnetization tends to be unstable at both ends of the free magnetic layer 25 in the track width direction. However, both ends of the free magnetic layer 25 in the track width direction are disposed near the hard bias layers 28. Therefore a large compressive stress is applied to both ends of the free magnetic layer 25 in the track width direction. Accordingly, the anisotropy due to the magnetoelastic effect is increased at both ends of the free magnetic layer 25 in the track width direction, thereby stabilizing the magnetization direction.

Accordingly, even if the longitudinal bias magnetic field is decreased by reducing the thickness of the hard bias layers 28, the free magnetic layer 25 can be a stable single domain. Decreasing the longitudinal bias magnetic field by reducing the thickness of the hard bias layers 28 can stabilize magnetization pinning of the pinned magnetic layer 23 in the height direction.

Since the compressive stress at the center of the free magnetic layer 25 is smaller than the compressive stress at both ends of the magnetic layer 25, the decreasing of the detection sensitivity of the magnetic field can be suppressed.

The magnetostriction constant λ of the free magnetic layer 25 is preferably in the range of $-0.5\times10^{-6}\geq\lambda\geq-8\times10^{-6}$. The thickness t of the hard bias layers 28 is preferably in the range of 200 Å≥t≥100 Å. Too small a magnetostriction constant λ of the free magnetic layer 25 or too large a thickness t of the hard bias layers 28 decreases the reproducing sensitivity of the magnetic sensor. On the other hand, too large a magnetostriction constant λ of the free magnetic layer 25 or too small a thickness t of the hard bias layers 28 tends to generate the disorder in reproducing waveforms of the magnetic sensor.

The magnetic sensors of the present embodiments shown in Fig. 1, Fig. 9, and Fig. 10 are manufactured by forming thin films by sputtering or vapor deposition, and patterning by resist photolithography. In sputtering and resist photolithography, known methods for forming a magnetic sensor are used.

In order to overlap the atoms in the first magnetic sublayer 23a and the atoms in the nonmagnetic metal layer 22 or in the interlayer 40, and to generate deformations in each crystal structure, the nonmagnetic metal layer 22 or the interlayer 40, and the first magnetic sublayer 23a are preferably deposited under, for example, the following conditions.

DC magnetron sputtering

Input electric power to targets: 10 to 100 W

Ar pressure: 0.01 to 0.5 Pa

Distance between the targets and a substrate: 100 to 300 mm

When the magnetic sensor shown in Fig. 1 is formed, the temperature of the substrate in depositing the first magnetic sublayer 23a is higher than that in depositing the nonmagnetic metal layer 22. In this case, a larger deformation can be generated by the effect of thermal expansion.

The magnetic sensor in Fig. 1 in which the hard bias layers 28 are disposed at both sides of the multilayer film T1 is formed. Then, the magnetizations of the first magnetic sublayer 23a, the second magnetic sublayer 23c, and the hard bias layers 28 are directed in the height direction by applying a strong magnetic field, for example, 1,200 (kA/m) in the height direction. Then the applied magnetic field is controlled to be smaller than the spin flop magnetic field of the first magnetic sublayer 23a and the second magnetic sublayer 23c. Thus, the magnetizations of the first magnetic sublayer 23a and the second magnetic sublayer 23c are

directed in antiparallel directions. The magnetic field in the height direction is removed, and then a magnetic field larger than the coercive force of the hard bias layers 28 is applied in the track width direction to magnetize the hard bias layers 28.

When the magnetic field in the track width direction is removed, the magnetizations of the first magnetic sublayer 23a and the second magnetic sublayer 23c of the pinned magnetic layer 23 are directed in the directions antiparallel or parallel with respect to the height direction mainly by the magnetoelastic effect. The free magnetic layer 25 is put into a single magnetic domain state in the track width direction by the longitudinal bias magnetic field from the hard bias layers 28.

An induced anisotropy may be added to the first magnetic sublayer 23a and the second magnetic sublayer 23c of the pinned magnetic layer 23 by applying a magnetic field in the height direction during deposition of the pinned magnetic layer 23.

However, when the optical track width of the pinned magnetic layer 23 is 0.15 μm or less, the magnetoelastic effect becomes very large. In particular, according to the present invention, the magnetostriction constants λ of the first magnetic sublayer 23a and the second magnetic sublayer 23c and the compressive stress in the track width direction applied to the multilayer film are increased. Therefore, the magnetization of the pinned magnetic layer 23 is mainly pinned by the magnetoelastic effect.

According to the present embodiments, layered products composed of the hard bias layers 28 and the electrode layers 29 are formed at both sides of the multilayer film T1 or T2. These layered products apply the compressive stress to the multilayer film T1 or T2. However, at both sides of the multilayer film T1 or T2, the hard bias layers 28 are not always required. For example, layered products composed of a soft magnetic layer and an antiferromagnetic layer may be disposed at both sides of the multilayer film T1 or T2. Alternatively, an insulating layer may be disposed at both sides of the multilayer film T1 or T2.

The magnetic sensor according to the present invention may be used as a magnetic sensor in which the sense current flows in the direction perpendicular to the thickness of the multilayer film T1 or T2, for example, a tunneling magnetoresistive element or a current perpendicular to plane giant magnetoresistive (CPP-GMR) magnetic sensor. In this case, the electrode layers are formed on the multilayer film T1 or T2 and under the multilayer film T1 or T2.

Although preferable embodiments of the present invention were described above, various modifications can be added as long as the modifications do not deviate from the scope of the present invention.

The embodiments described above exemplify the present invention, which are not served to limiting the appended claims of the present invention.

EXAMPLES

The following multilayer films were formed and were

annealed at 290°C for four hours. Then each of the magnetostriction was measured.

silicon substrate/ alumina (1,000 Å)/ $(Ni_{0.8}Fe_{0.2})_{60}Cr_{40}$ (52 Å)/ nonmagnetic metal layer (underlayer)/ pin 1/ Ru (9 Å)/ pin 2 (40 Å)/ Cu (85 Å)/ Ta (30 Å)

According to this Example, for example, the second magnetic sublayer, the nonmagnetic conductive layer, and the free magnetic layer are not formed, thereby accurately measuring the magnetostriction of the first magnetic sublayer 23a. The nonmagnetic metal layer (i.e., underlayer) is composed of Ru or $Pt_{50}Mn_{50}$ (atomic percent); a pin 1 is composed of Co, $Co_{90}Fe_{10}$ (atomic percent), or $Fe_{50}Co_{50}$ (atomic percent); and a pin 2 is composed of Co or $Co_{90}Fe_{10}$ (atomic percent). Hereinafter, the $Co_{90}Fe_{10}$ (atomic percent) is referred to as "CoFe" and the $Fe_{50}Co_{50}$ (atomic percent) is referred to as "FeCo".

The magnetostriction was measured by a bending method. In the bending method, the multilayer film is incurvated to form a uniaxial deformation. The magnetostriction constant is measured using the change of the uniaxial anisotropy due to the inverse magnetostrictive effect.

Fig. 11 shows the results. According to the results of this experiment, in both cases where the nonmagnetic metal layer is composed of Ru and where the nonmagnetic metal layer is composed of $Pt_{50}Mn_{50}$ (atomic percent), the magnetostriction constant of the multilayer film having the pin 1 composed of Co or FeCo is larger than that of the multilayer film having the pin 1 composed of CoFe. Even if a deformation is

generated in CoFe, the magnetostriction is not changed so much, compared with Co and FeCo. This seems to be the reason for the above results.

The multilayer film that includes the nonmagnetic metal layer has a magnetostriction constant larger than that of the multilayer film that does not include the nonmagnetic metal layer.

In the multilayer film having the pin 1 composed of Co, the increases of the magnetostriction constant are almost the same between the multilayer film having the nonmagnetic metal layer composed of Ru and the multilayer film having the nonmagnetic metal layer composed of $Pt_{50}Mn_{50}$ (atomic percent).

When the multilayer film has the pin 1 composed of Co or FeCo, in the area where the thickness of the nonmagnetic metal layer is about 5 Å or more, as the thickness increases, the magnetostriction constant is gradually decreased. This is because a large thickness of the nonmagnetic metal layer readily allows the boundary face between the nonmagnetic metal layer and the pin 1 to be mismatched. To the contrary, a small thickness of the nonmagnetic metal layer readily allows the lattice constant of the nonmagnetic metal layer to be changed. Therefore, the nonmagnetic metal layer and the pin 1 are readily matched at the boundary face while having deformations.

CLAIMS

1. A magnetic sensor comprising a pinned magnetic layer, a free magnetic layer, and a nonmagnetic conductive layer disposed therebetween,

wherein the pinned magnetic layer comprises a plurality of laminated magnetic sublayers having a nonmagnetic interlayer therebetween;

a first magnetic sublayer of the plurality of the magnetic sublayers is disposed farthest from the nonmagnetic conductive layer, and is in contact with a nonmagnetic metal layer comprising at least one element selected from the group consisting of Ru, Re, Os, Ti, Rh, Ir, Pd, Pt, and Al;

the crystals in the nonmagnetic metal layer and the crystals in the first magnetic sublayer are oriented in an epitaxial or a heteroepitaxial state; and

an end face of the pinned magnetic layer is opened, the end face opposing a face of a recording medium.

2. The magnetic sensor according to claim 1,

wherein the nonmagnetic metal layer comprises at least one element selected from the group consisting of Rh, Ir, Pd, Pt, and Al; and

the nonmagnetic metal layer has a face-centered cubic (fcc) lattice structure in the vicinity of a boundary face adjacent to the first magnetic sublayer of the pinned magnetic layer or in the entire areas of the nonmagnetic metal layer, an equivalent crystal plane represented by a

{111} plane being preferentially oriented in the direction parallel to the boundary face.

3. The magnetic sensor according to claim 1,

wherein the nonmagnetic metal layer comprises at least one element selected from the group consisting of Ru, Re, Os, and Ti; and

the nonmagnetic metal layer has a hexagonal close-packed (hcp) structure in the vicinity of a boundary face adjacent to the first magnetic sublayer of the pinned magnetic layer or in the entire areas of the nonmagnetic metal layer, a C-plane ({0001} plane) being preferentially oriented in the direction parallel to the boundary face.

4. The magnetic sensor according to claim 1, further comprising:

bias layers to supply the free magnetic layer with a longitudinal bias magnetic field, the bias layers being disposed at both side ends of the free magnetic layer and the pinned magnetic layer.

5. The magnetic sensor according to claim 1, wherein the first magnetic sublayer of the pinned magnetic layer has a face-centered cubic (fcc) lattice structure in the vicinity of a boundary face adjacent to the nonmagnetic metal layer or in the entire areas of the first magnetic sublayer, an equivalent crystal plane represented by a {111} plane being preferentially oriented in the direction parallel to the

boundary face.

6. The magnetic sensor according to claim 5, wherein the first magnetic sublayer of the pinned magnetic layer comprises Co or Co_xFe_y ($20 \geq y$, $x+y=100$, and wherein each of x and y is represented as an atomic percent).

7. The magnetic sensor according to claim 1, wherein the first magnetic sublayer of the pinned magnetic layer has a body-centered cubic (bcc) lattice structure in the vicinity of a boundary face adjacent to the nonmagnetic metal layer or in the entire areas of the first magnetic sublayer, an equivalent crystal plane represented by a {110} plane being preferentially oriented in the direction parallel to the boundary face.

8. The magnetic sensor according to claim 7, wherein the first magnetic sublayer of the pinned magnetic layer comprises Co_xFe_y ($y \geq 20$, $x+y=100$, and wherein each of x and y is represented as an atomic percent).

9. The magnetic sensor according to claim 1,

wherein the first magnetic sublayer of the pinned magnetic layer has a face-centered cubic (fcc) lattice structure in the vicinity of a boundary face adjacent to the nonmagnetic metal layer, an equivalent crystal plane represented by the {111} plane being preferentially oriented in the direction parallel to the boundary face; and

the first magnetic sublayer of the pinned magnetic layer has a body-centered cubic (bcc) lattice structure in the vicinity of a boundary face adjacent to the nonmagnetic interlayer, an equivalent crystal plane represented by the {110} plane being preferentially oriented in the direction parallel to the boundary face.

10. The magnetic sensor according to claim 9,

wherein the first magnetic sublayer of the pinned magnetic layer comprises Co_xFe_y ($20 \geq y$, $x+y=100$, and wherein each of x and y is represented as an atomic percent) or Co in the vicinity of the boundary face adjacent to the nonmagnetic metal layer; and

the first magnetic sublayer of the pinned magnetic layer comprises Co_xFe_y ($y \geq 20$, $x+y=100$, and wherein each of x and y is represented as an atomic percent) in the vicinity of the boundary face adjacent to the nonmagnetic interlayer.

11. The magnetic sensor according to claim 10, wherein iron content in the first magnetic sublayer of the pinned magnetic layer gradually increases from the boundary face adjacent to the nonmagnetic metal layer to the boundary face adjacent to the nonmagnetic interlayer.

12. The magnetic sensor according to claim 1, wherein a value calculated by dividing the difference between the nearest interatomic distance of the nonmagnetic metal layer in the plane parallel to a boundary face and the nearest

interatomic distance of the first magnetic sublayer of the pinned magnetic layer in the plane parallel to the boundary face by the nearest interatomic distance of the first magnetic sublayer is in the range of 0.05 to 0.20.

13. The magnetic sensor according to claim 1, further comprising:

an interlayer disposed between the nonmagnetic metal layer and the first magnetic sublayer of the pinned magnetic layer, the interlayer comprising PtMn alloy or X-Mn alloy (wherein X is at least one element selected from the group consisting of Pd, Ir, Rh, Ru, Os, Ni, and Fe).

14. The magnetic sensor according to claim 13,

wherein the crystals in the nonmagnetic metal layer and the crystals in the interlayer are oriented in an epitaxial state; and

the crystals in the interlayer and the crystals in the pinned magnetic layer are oriented in an epitaxial or a heteroepitaxial state.

15. The magnetic sensor according to claim 1, wherein the first magnetic sublayer comprises a magnetic material having a positive magnetostriction constant.

16. The magnetic sensor according to claim 1, further comprising:

electrode layers disposed at both sides of the free

magnetic layer, the nonmagnetic conductive layer, and the pinned magnetic layer, the electrode layers comprising Cr, α-Ta, or Rh.

17. The magnetic sensor according to claim 16, wherein the distance between the crystal planes of the electrode layers comprising Cr in the direction parallel to the layers is 0.2044 nm (the distance between the {110} planes in the bcc structure) or more; the distance between the crystal planes of the electrode layers comprising α-Ta in the direction parallel to the layers is 0.2337 nm (the distance between the {110} planes in the bcc structure) or more; or the distance between the crystal planes of the electrode layers comprising Rh in the direction parallel to the layers is 0.2200 nm (the distance between the {111} planes in the fcc structure) or more.

18. The magnetic sensor according to claim 1, wherein an optical track width of the pinned magnetic layer is 0.15 μm or less.

19. A magnetic sensor as hereinbefore described with reference to the accompanying drawings.

Application No: GB 0401758.8 **Examiner:** Ralph Cannon
Claims searched: All **Date of search:** 29 March 2004

Patents Act 1977 : Search Report under Section 17

Documents considered to be relevant:

Category	Relevant to claims	Identity of document and passage or figure of particular relevance	
X	1, 4, 16	US 20020044398 A1	(SASAKI), in particular figs 1, 21 and paragraphs 70, 71, 77, 176-187
A		US 5648885	(NISHIOKA) fig. 8 col. 7 line 60 - col. 10 line 39.
A		US 5920446	(GILL) fig. 4, col. 3 line 30 - col. 4 line 21 col. 5 line 40 - col. 6 line 40

Categories:

X	Document indicating lack of novelty or inventive step	A	Document indicating technological background and/or state of the art
Y	Document indicating lack of inventive step if combined with one or more other documents of same category	P	Document published on or after the declared priority date but before the filing date of this invention
&	Member of the same patent family	E	Patent document published on or after, but with priority date earlier than, the filing date of this application

Field of Search:

Search of GB, EP, WO & US patent documents classified in the following areas of the UKC[W]:

G5R

Worldwide search of patent documents classified in the following areas of the IPC[7]:

G11B, G01R

The following online and other databases have been used in the preparation of this search report:

Online: EPODOC, WPI, PAJ